Science & Technology Development Journal 2025, 28(3):3786-3794

Open Access Full Text Article

Research Article

Effect of electrospinning parameters on the morphology of polyurethane nanofibers and their shape memory behaviors

Thi Thu Thuy Nguyen[1,*], Thi Le Le[1], Ngoc Phan Vu[2]

ABSTRACT

Introduction: We investigated the effect of various electrospinning parameters on the morphology and average diameter of shape memory polyurethane (PU) nanofibers. The shape memory performance of an electrospun PU nanofiber mat was also studied.

Methods: The examined parameters included solution concentration (16–22 wt%), applied voltage (8–10 kV), feed rate (0.8–1.2 mL/h), needle-to-collector distance (18–20 cm), and solvent mixture (*N*,*N*-dimethylformamide (DMF), DMF/chloroform, and DMF/ethyl acetate). The morphology of electrospun PU nanofibers was observed using a scanning electron microscope. The shape memory properties of the electrospun PU nanofiber mat obtained at the optimal parameters were investigated using a thermomechanical cyclic testing program.

Results: Bead-free nanofibers with an average diameter of 600 nm were obtained using a 20 wt% PU solution in DMF, an applied voltage of 10 kV, a feed rate of 1.0 mL/h, and a needle-to-collector distance of 20 cm. Using DMF/chloroform and DMF/ethyl acetate as solvents, uniform PU nanofibers were obtained at a PU concentration of 16 wt%. The electrospun PU nanofiber mat exhibited excellent shape memory properties, achieving shape recovery ratios and shape fixity ratios exceeding 90%.

Conclusions: PU nanofiber mats were successfully fabricated by the electrospinning method and it is considered as a potential material for shape memory applications.

Key words: shape memory, nanofibers, polyurethane, electrospinning, thermomechanical cyclic testing

[1]*Phenikaa University Nano Institute, Phenikaa University, Ha Dong district, Hanoi, Việt Nam*

[2]*Faculty of Biological, Chemical and Environmental Engineering, Phenikaa University, Ha Dong district, Hanoi, Việt Nam*

Correspondence

Thi Thu Thuy Nguyen, Phenikaa University Nano Institute, Phenikaa University, Ha Dong district, Hanoi, Việt Nam

Email: thuy.nguyenthithu@phenikaa-uni.edu.vn

History

- Received: 04-02-2025
- Revised: 17-04-2025
- Accepted: 10-06-2025
- Published Online: 05-09-2025

DOI :

https://doi.org/10.32508/stdj.v28i3.4424

INTRODUCTION

Shape memory polymers (SMPs) are smart materials that can transition between temporary and permanent shapes upon applying stimuli such as heat, light, pH, electricity, magnetic fields, and solvents [1–3]. The permanent shape is determined by crosslinking points formed through covalent bonds or physical interactions among molecules within the polymer network. The temporary shape is stabilized by weaker interactions between polymer chains or switching segments, which may include crystalline, liquid crystalline, or amorphous phases [4]. Thermoresponsive SMPs are the most widely researched SMPs, with their shape memory mechanism activated by heating to above their transition temperature, namely the glass transition temperature for thermoset SMPs and the melting temperature for thermoplastic SMPs [5]. Among the thermoresponsive SMPs, shape memory polyurethane (PU) exhibits advantageous characteristics, such as a wide range of shape recovery temperatures, good processability, biocompatibility, and high strain recovery capabilities. These attributes make PU-based SMPs suitable for use as biomaterials and in medical applications, including sensing, actuation, scaffold construction, and artificial blood vessels [6–10]. PU is a multiblock copolymer with excellent thermal shape memory properties resulting from the phase-separated structure of its hard and soft segments [11]. The hard segments form physical crosslinks through polar interactions, hydrogen bonding, and crystallization within the hard domains. The soft segments, typically derived from long-chain diols such as polyester or polyether polyols, facilitate reversible movement. The thermally responsive soft segment of PU enables shape recovery upon reaching the transition temperature (Ttrans). Lv et al. [12] reported that electrospun microfibers based on polyurethane (SMPU) possess excellent biocompatibility and shape memory characteristics, demonstrating promising biomedical applications. Notably, the incorporation of hydroxyapatite (HA) into SMPU microfibers reduces the fiber diameter, which positively impacts the shape memory functionality of the composite membrane. The original morphology of SMPU/HA microfibers is restored in just 6 seconds at a temperature of 40 °C. Polyesterurethane nanofibers with an average diameter ranging from 1.8 to 3.1 μm have been prepared

Cite this article : Nguyen T T T, Le T L, Vu N P. **Effect of electrospinning parameters on the morphology of polyurethane nanofibers and their shape memory behaviors**. *Sci. Tech. Dev. J.* 2025; 28(3):3786-3794.

by electrospinning in another study[13]. The resulting fiber mats exhibited good shape memory properties, demonstrating shape recovery ratios of 89–95% and shape fixity ratios of 82–83% after the second cycle when subjected to minor deformations at body temperature. Another study reported that incorporating graphene oxide into SMPU nanofibers enhanced the fiber surface morphology and shape memory performance, with average fixity and recovery ratios of 92.1% and 96.5%, respectively[14].

Electrospinning is a versatile technique for producing nanofibers with diameters from nanometers to micrometers. The nanofiber morphology and diameter can be controlled by adjusting both solution parameters (molecular weight, concentration, viscosity, conductivity, surface tension, and dielectric constant) and process parameters (voltage, feed rate, needle-to-collector distance, and needle diameter)[15,16]. Zhuo et al.[17] fabricated PU nanofibers via electrospinning, yielding fiber diameters ranging from 50 to 700 nm. They demonstrated that a solution concentration was a primary determinant in the electrospinning process, influencing the transformation of the polymer solution into ultrafine fibers under an applied voltage and feed rate of 12 kV and 0.08 mL/min, respectively. Differential scanning calorimetry (DSC) results indicated that the prepared nanofibers possessed the structural characteristics required for shape memory behavior. Banikazemi et al. investigated electrospun nanofibers of ε-caprolactone-based PU and found that solution concentration and solvent system significantly influenced the nanofiber diameter, whereas voltage, feed rate, and needle-to-collector distance had relatively little effect[18]. Fibrous SMPs exhibit desirable characteristics, including a large specific surface area, high porosity, and excellent permeability. These properties enable increased chain mobility, thereby reducing the transition temperature and enhancing the shape memory effect. Specifically, SMP nano/microfibers have been reported to exhibit superior shape memory properties to shape memory films[19,20]. This has been attributed to their large surface area accelerating heating and cooling, thereby improving shape memory efficiency. The effect of the nanofiber structure, including the fiber diameter and morphology, on shape memory properties and their applications has been studied[12,13,21–23]. Sauter et al.[23] rrevealed a correlation between the fiber diameter and the shape memory performance of electrospun PU membranes. Fibers with nanoscale diameters enhanced the shape memory properties due to improved molecular alignment with the fiber elongation direction and increased stress generation within fibers of smaller diameters.

In this study, we systematically investigated the effects of various parameters, including solution concentration, solvent, voltage, feed rate, and needle-to-collector distance, on the morphology and average diameter of PU nanofibers fabricated by electrospinning. Additionally, the shape memory properties of a PU nanofiber mat obtained at the optimal fabrication parameters was explored.

MATERIALS AND METHODS

Materials

PU pellets (NEOTHANE®4095AP) were purchased from Dongsung Chemical NEOTHANE® (Korea). DMF, ethyl acetate (EA), and chloroform were supplied by Samchun Chemicals Co., Ltd. (Korea). All chemicals were used without further purification.

Preparation of electrospun PU nanofibers

Various PU solutions were prepared by dissolving PU pellets in different solvent systems: DMF, DMF/chloroform (with ratios of 80/20, 60/40, and 40/60), and DMF/EA (with ratios of 80/20, 60/40, and 40/60). The solution concentrations were 16, 18, 20, and 22 wt%. The prepared solutions were loaded into a 5-mL plastic syringe with a stainless-steel needle. The syringe was placed in an infusion pump with the feed rate ranging from 0.8 to 1.2 mL/h. The distance from the needle tip to the collector was varied between 16 and 20 cm. An electrical field was applied at a voltage of 8, 9, or 10 kV.

Characterization of electrospun PU nanofibers

Scanning electron microscopy (SEM; JSM-6510LV) was used to examine the effect of the polymer solution and processing parameters on the PU nanofiber morphology. The nanofiber diameter distribution was determined by measuring approximately 50 randomly selected nanofibers in SEM images using ImageJ software.

The melting and crystallization behaviors of the PU pellets and electrospun PU nanofibers were characterized using DSC (204F1 Phoenix, Netzsch). Measurements were conducted in a temperature range of −34 to 250 °C at a heating rate of 10 °C/min.

Shape memory property of electrospun PU nanofiber mat

The shape memory properties of an electrospun PU nanofiber mat were investigated using a thermomechanical cyclic testing program. Samples were subjected to deformation and recovery cycles performed

by controlling the temperature of air circulating in an oven. In each cycle, the sample was first heated to 80 °C for 5 minutes, then deformed by stretching to a predetermined strain. The temporary shape was then fixed by cooling the sample to 5 °C for 2 minutes in a refrigerator. Shape recovery was induced by reheating the sample to 80 °C for 2 minutes. This cycle was repeated five times. The shape memory behavior was recorded using a digital camera attached to a fluorescence stereomicroscope (M165 FC, Leica).

To evaluate the shape memory effect, the ratios of shape fixity (Rf) and shape recovery (Rr) were quantified as follows:

$$R_r(N) = \frac{\varepsilon_m(N)-\varepsilon_f(N)}{\varepsilon_m(N)-\varepsilon_f(N-1)} \times 100 \quad (1)$$

$$R_f(N) = \frac{\varepsilon_u}{\varepsilon_m} \times 100 \quad (2)$$

where ε_m is the maximum strain length, ε_u is the strain length at 5 °C, ε_f is the length after shape recovery, and N is the number of cycles[7,13].

RESULTS

Morphology of PU nanofibers prepared at different solution concentrations

The concentration of the polymer solution significantly influenced the fiber formation and morphology during PU electrospinning. Figure 1 shows SEM images and the average fiber diameter of PU nanofibers prepared from PU solutions with different concentrations in the DMF solvent. The applied voltage was 10 kV, the feed rate was 1.0 mL/h, and the needle-to-collector distance was 20 cm.

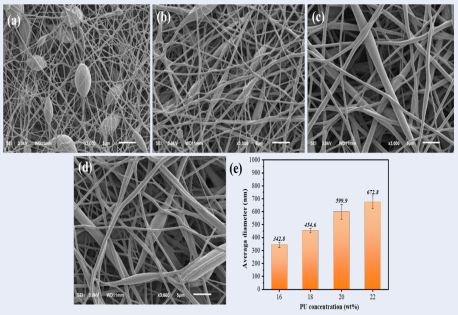

Figure 1: SEM images of PU nanofibers prepared at different concentrations: (a) 16 wt%, (b)18 wt%, (c) 20 wt%, (d) 22 wt%, and (e) the average diameter of nanofibers

The images of the nanofibers prepared at PU concentrations of 16 and 18 wt% revealed bead formation (Figure 1 a-b). The nanofiber diameter increased with increasing PU concentration, with average fiber diameters of 343, 455, 600, and 673 nm obtained at concentrations of 16, 18, 20, and 22 wt%, respectively. Based on the SEM analysis of the electrospun fibers, a PU solution concentration of 20 wt% was selected for subsequent investigations.

Morphology of PU nanofibers prepared at different voltages

The morphology and average diameter of PU nanofibers fabricated at voltages of 8, 9, and 10 kV are shown in Figure 2. The PU concentration in the DMF solvent was 20 wt%, the feed rate was 1.0 mL/h, and the needle-to-collector distance was 20 cm. PU nanofibers were readily produced at all three voltages, with the average diameter decreasing slightly with increasing voltage; diameters of 785, 684, and 600 nm were obtained at voltages of 8, 9, and 10 kV, respectively. A voltage of 10 kV was chosen in subsequent experiments.

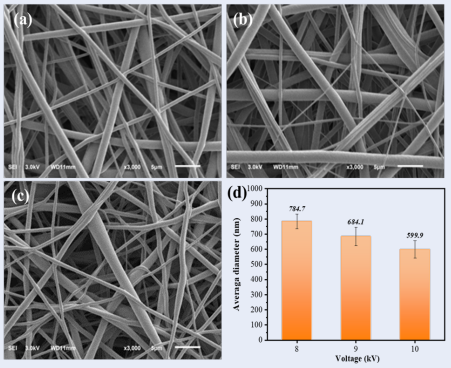

Figure 2: SEM images of PU nanofibers prepared at voltages of (a) 8 kV, (b) 9 kV, and (c) 10 kV; (d) average diameter of the nanofibers

Morphology of PU nanofibers prepared at different feed rates

The effect of the solution feed rate (0.8, 1.0, and 1.2 mL/h) on the morphology and average diameter of the PU nanofibers was observed by SEM (Figure 3). ThePU concentration in the DMF solvent was 20 wt%, the voltage was 10 kV, and the needle-to-collector dis- tance was 20 cm. The average fiber diameter increased with increasing feed rate and was 579, 600, and 693 nm at feed rates of 0.8, 1.0, and 1.2 mL/h, respec- tively. SEM analysis demonstrated the successful pro- duction of PU nanofibers across the range of solution feed rates. A feed rate of 1.0 mL/h was selected for further investigation.

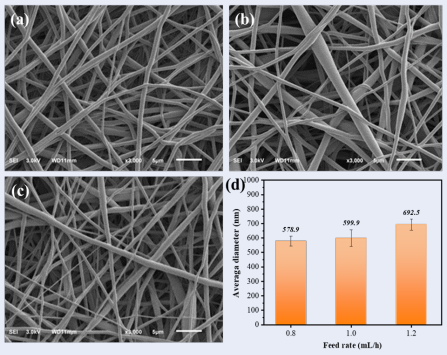

Figure 3: SEM images of PU nanofibers prepared at feed rates of (a) 0.8 mL/h, (b) 1.0 mL/h, and (c) 1.2 mL/h; (d) average diameter of the nanofibers

Morphology of PU nanofibers prepared at different needle-to-collector distances

The effect of the needle-to-collector distance (16, 18, and 20 cm) on the morphology and average fiber diameter is shown in Figure 4. The nanofibers were fabricated at a PU concentration of 20 wt% in the DMF solvent, the voltage was 10 kV, and the feed rate was 1.0 mL/h. Little variation was observed in the average fiber diameter, with diameters of 552, 571, and 600 nm obtained at distances of 16, 18, and 20 cm, respectively. However, the morphology changed from beaded nanofibers to uniform nanofibers with increasing needle-to-collector distance. Therefore, the appropriate needle-to-collector distance for PU nanofiber formation was considered to be 20 cm.

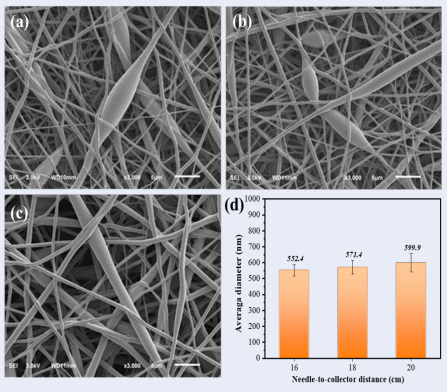

Figure 4: SEM images of PU nanofibers prepared at needle-to-collector distances of (a) 16 cm, (b) 18 cm, and (c) 20 cm; (d) average diameter of the nanofibers

Morphology of PU nanofibers prepared in different solvent systems

The type of solvent affects the solubility, viscosity, surface tension, and conductivity of the polymer solution, which in turn affects the formability and morphology of the obtained fibers. While PU exhibits good solubility in DMF, low PU concentrations (e.g., 16 wt%) resulted in beaded nanofibers (Figure 1-a). Figure 5 shows SEM images of 16 wt% PU nanofibers fabricated with different solvent mixtures and ratios, a feed rate of 1.0 mL/h, a voltage of 10 kV, and a needle-to-collector distance of 20 cm. The addition of co-solvents, such as chloroform or EA, changed some important properties of the solutions, including surface tension, viscosity, and volatility, which improved the fiber morphology.

Shape memory behavior of electrospun PU membrane

The electrospun PU membrane used in the shape memory test was prepared at a PU solution concentration of 20 wt% in DMF, a voltage of 10 kV, a feed rate of 1.0 mL/h, and a needle-to-collector distance of 20 cm. Thermally triggered PU typically undergoes thermal transitions, such as those at the glass transition temperature (T_g) and melting temperature (T_m), for shape recovery. Figure 6 shows DSC curves of a PU pellet and the electrospun PU membrane. The PU pellet exhibited T_m of 73.13 °C, while the PU membrane had a higher T_m of 85.19 °C.

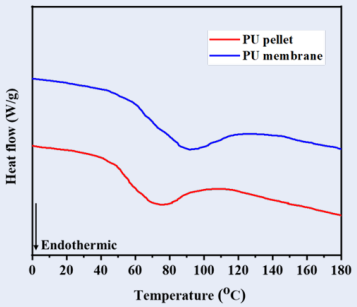

Figure 6: DSC curves of PU pellet and electrospun PU membrane

To investigate the shape memory properties of the electrospun PU membrane, it was elongated at 80 °C, unloaded, and evaluated for shape recovery. Figure 7 shows the shape fixity and shape recovery ratios obtained from five thermomechanical cycles performed on the membrane.

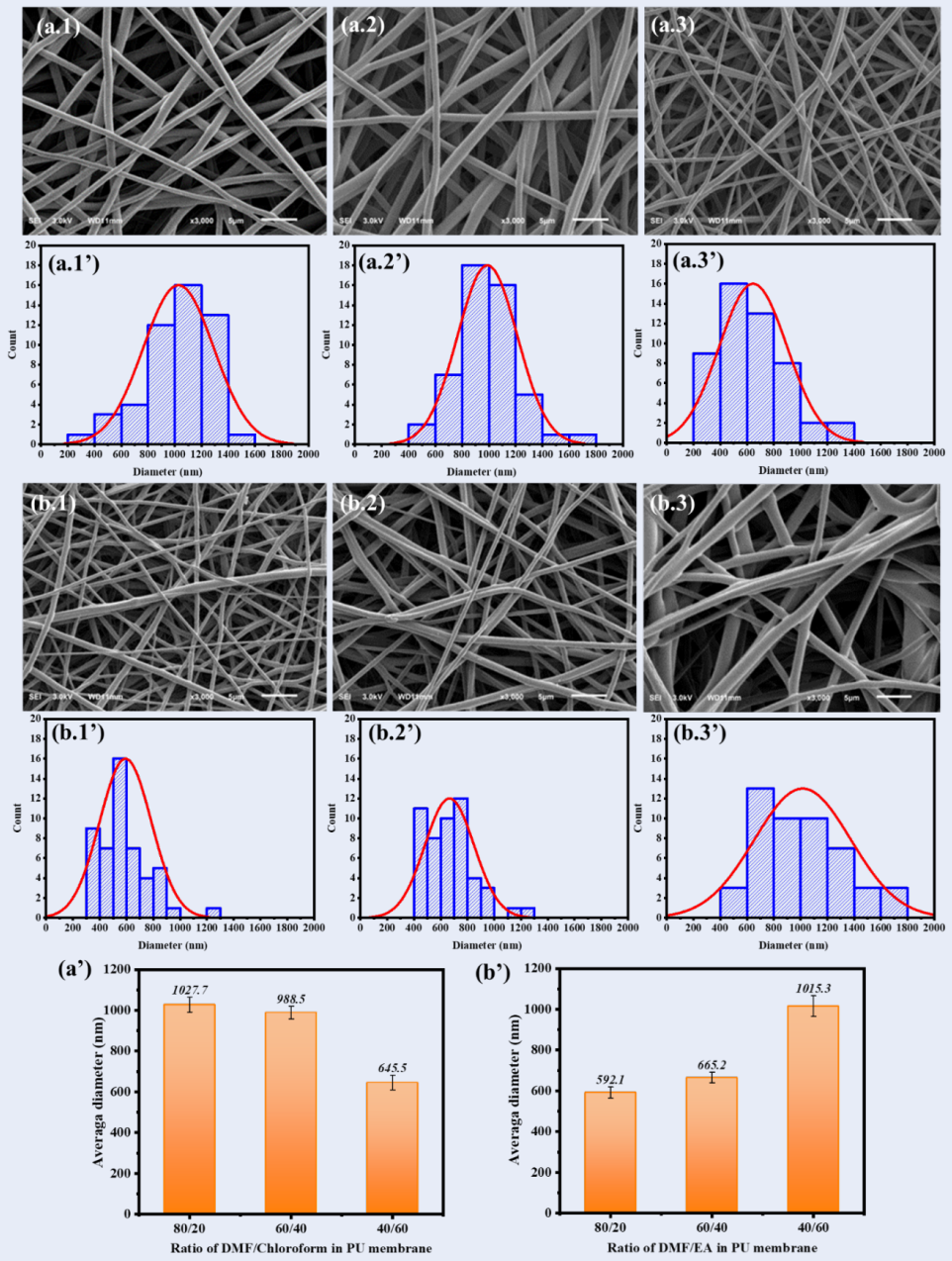

Figure 5: SEM images and diameter distributions of PU nanofibers fabricated with different solvent mixtures and ratios: (a.1 and a.1') DMF/chloroform = 80/20, (a.2 and a.2') DMF/chloroform = 60/40, (a.3 and a.3') DMF/chloroform = 40/60, (b.1 and b.1') DMF/EA = 80/20, (b.2 and b.2') DMF/EA = 60/40, and (b.3 and b.3') DMF/EA = 40/60; (a', b') average diameter of the PU nanofibers

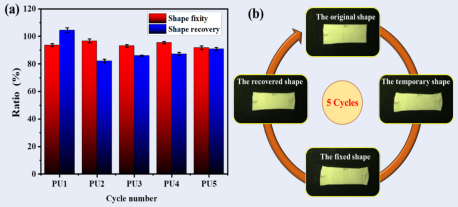

Figure 7: Shape fixity and shape recovery ratios of electrospun PU membrane (a); shape memory cycle of the membrane (b)

DISCUSSION

Effect of parameters on morphology of PU nanofibers

The effect of the solution concentration on the fiber morphology is attributed to positive correlation between the concentration and viscosity of the polymer solution. The SEM images of nanofibers prepared at PU concentrations of 16 and 18 wt% revealed bead formation rather than continuous fibers because of the low viscosity at these concentrations (Figure 1a-b). The polymer chains underwent limited entanglement, leading to the formation of droplets under the pulling effect of the electric field. At a PU concentration of 20 wt%, continuous and uniform nanofibers with a smooth morphology were observed without droplet formation (Figure 1-c). However, a concentration exceeding 20 wt% resulted in excessive viscosity, impeding fiber formation, as the PU solution solidified in the nozzle tip, clogging the nozzle. Elevated viscosity also enhanced the entanglement of polymer chains, resulting in an increased fiber diameter, consistent with the previously reported trend[24].

Electrospinning requires a sufficient applied voltage to overcome the surface tension of the solution and initiate fiber formation. Increasing the voltage from 8 kV resulted in a smaller fiber size and a more uniform diameter distribution. This can be explained by the larger electric field generating a greater pulling force. However, an excessively high voltage led to an unstable spinning process and the formation of irregular-sized and fractured fibers. In contrast, when the voltage was insufficient to overcome the surface tension of the solution and stabilize the jet, beads or beaded fibers were formed[25].

The average fiber diameter increased with the feed rate in the range of 0.8 to 1.2 mL/h. At the lowest feed rate (0.8 mL/h), insufficient solution delivery to the nozzle tip resulted in a discontinuous electrospinning process. In contrast, at the highest feed rate (1.2 mL/h), greater fiber adhesion was observed, likely due to incomplete solvent evaporation as the solution jet traveled from the syringe needle to the collector. Cay et al. found that an increased feed rate led to considerable polymer deposition on the collector in a short time, forming a conjunction of nanofibers, which subsequently increased the fiber diameter[24]. A feed rate of 1.0 mL/h ensured continuous solution delivery without premature solidification at the nozzle, resulting in PU nanofibers with a narrow diameter distribution and an average diameter of 600 nm.

The needle-to-collector distance had little effect on the average fiber diameter, although the fiber morphology was significantly influenced. At the shortest distance of 16 cm, a strong pulling force was exerted on the solution, and the incomplete solvent evaporation resulted in the formation of a wet fiber membrane on the collector. Increasing the distance to 18 cm facilitated fiber formation, but some interfiber adhesion persisted because the solvent had not completely evaporated. At a distance of 20 cm, uniform, continuous fibers without adhesion were obtained (Figure 4-c).

The solvent concentration also affected the electrospinning process. At the lowest PU concentration of 16 wt% in DMF, nonuniform and beaded fibers were produced, resulting in insufficient entanglement between PU molecular chains. Consequently, the extensional forces exerted on the electrospinning jet were not adequately resisted by intermolecular interactions, leading to jet breakup. Furthermore, the high surface tension of DMF contributed to bead formation by thermodynamically favoring a reduction in surface area per unit mass, driving the jets into spherical droplets[26]. Increasing the PU solution concentration to 20 wt% led to increased solution viscosity, promoting greater entanglement between polymer chains, stabilizing the stretching jet against breakup, and forming uniform nanofibers.

The use of DMF/chloroform solvent mixtures with a PU concentration of 16 wt% increased the solution viscosity, facilitating the production of continuous and bead-free nanofibers. Additionally, the lower surface tension of chloroform compared with DMF (Table 1) contributed to the formation of uniform nanofiber morphologies. Moreover, the average diameters of PU nanofibers fabricated using the mixed-solvent systems were larger than those prepared using DMF alone. This can be attributed to the lower conductivity and boiling point of chloroform and EA. The reduced conductivity decreased the concentration of

Table 1: Properties of the solvents used [26]

Solvent	Surface tension (mN/m)	Conductivity (μS/cm)	Boiling point (°C)
DMF	33.9	10.9	153.0
Chloroform	26.0	-	61.2
EA	22.7	0.29	77.1

charge carriers in the electrospinning jet, thereby reducing the electrostatic and Coulombic forces responsible for jet stretching. The lower boiling point (corresponding to higher volatility) led to more rapid solidification of the jet, hindering its elongation and resulting in larger fiber diameters. However, a 40/60 DMF/chloroform ratio resulted in excessive viscosity, preventing continuous solution ejection at 10 kV and forming dried solution droplets, causing blockage of the needle tip. The addition of EA to DMF produced uniform and bead-free nanofibers. Cay et al. [24] reported that EA can disrupt intermolecular forces, thereby increasing the solution viscoelasticity and facilitating fiber stretching. In their study, this effect was less pronounced at lower DMF ratios, resulting in larger fiber diameters. Moreover, EA has a very low dielectric constant, limiting electrospinnability at high concentrations [26]. The benefits of mixed-solvent systems for PU electrospinning have previously been reported [27,28] Properties of the solvents used.

Shape memory performance of electrospun PU membrane

The difference in T_m between the PU pellet and electrospun PU nanofibers indicates modification of the PU crystal structure during electrospinning. The micro-phase separation between soft and hard segments of a PU nanofiber mat has been reported to be greater than that in a PU pellet [29]. The increased crystallinity in PU nanofibers may be attributed to extensive molecular chain rearrangement and orientation during the stretching in electrospinning, leading to a more ordered structure and higher T_m. In this study, a recovery temperature of 80 °C, between the onset and peak melting temperatures, was chosen to achieve an optimal balance between two key factors. First, it provided sufficient thermal energy to enhance chain mobility and melt the reversible physical crosslinks (hydrogen bonding and crystalline segments) in the PU nanofibers, facilitating entropy-driven shape recovery. Second, it was below the peak melting temperature to prevent complete melting, which could compromise the structural integrity of the membrane. The electrospun PU nanofiber mat exhibited a high shape fixity ratio of nearly 100% across all five cycles, demonstrating excellent shape-fixing performance. Upon heating, substantial recovery was observed in all samples, with the first cycle showing an initial recovery of 104.4%. This slight recovery beyond the original shape can be attributed to the release of residual strains introduced during electrospinning. Specifically, electrospinning subjects polymer solution jets to high extensional deformation under a strong electrical field, resulting in the polymer matrix inside electrospun nanofibers being in a stretched nonequilibrium state with a high level of stored elastic strain energy [30]. In this study, stored energy in the PU nanofibers was released after heating, driving significant shape recovery in the first cycle. In the second cycle, the shape recovery of the PU nanofiber mat reached 82.1%. With subsequent cycles, the shape recovery efficiency gradually increased, stabilizing at approximately 90% by the fifth cycle. This iterative tensile and recovery process, coupled with thermal stimulation, enhanced molecular mobility within the PU polymer, facilitating gradual fiber reorientation and rearrangement at the microstructural level, leading to improved shape recovery with each cycle. The similar results observed in thermomechanical cyclic testing affirm that PU nanofiber mats exhibit a robust shape memory effect [31,32]. Owing to their good shape memory properties, PU nanofibers have potential applications including filtration materials, smart fiber-reinforced composites with damping capabilities, and biomedical devices. In a review of SMP nanofibers, electrospun polylactic acid nanofiber mats demonstrated Rf and Rr values exceeding 88% and 96%, respectively, over three cycles at 60 °C. The addition of lactic acid oligomer as a plasticizer in the polylactic acid nanofibers effectively lowered the switching temperature to slightly above body temperature (around 40 °C) while maintaining high Rf and Rr values [33]. Zhang et al. [34] reported Nafion/poly(ethylene oxide) (PEO) blend nanofibers with excellent shape memoryproperties, achieving Rf and Rr values over 90% at a switching temperature of 130 °C. Ai et al. investigated the memory effect of PU/PEO blend electrospun fibrous membranes in terms of both the morphological structure design and the PU/PEO blend ratio. A co-spun PEO and PU nanofiber membrane with 50

wt% PEO exhibited the optimal shape memory effect. This was attributed to the extensive blend interface in individual fibers and sufficient fusion points between fibers, leading to a synergistic effect between the two components[35]. Current research aimed at enhancing the shape memory efficiency of polymer nanofiber membranes and tailoring the switching temperature for specific applications primarily focuses on the addition of nanofillers to the polymer network or the synthesis of novel copolymers[36].

CONCLUSIONS

We successfully fabricated PU nanofibers via electrospinning. The effect of key parameters, including polymer concentration, solvent system, applied voltage, feed rate, and needle-to-collector distance, on the average fiber diameter was investigated. Bead-free nanofibers with an average diameter of 600 nm were obtained using a 20 wt% PU solution in DMF solvent with a feed rate of 1 mL/h, an applied voltage of 10 kV, and a needle-to-collector distance of 20 cm. The addition of chloroform or EA as co-solvents resulted inbead-free nanofibers at a PU concentration of 16 wt%. The shape recovery and shape fixity ratios of an elec-trospun PU nanofiber mat were over 90% and 99%, respectively, after five cycles. These findings highlight the potential of electrospun PU nanofibers for shape memory applications.

COMPETING INTERESTS

The authors have no competing interests or personal relationships that could have appeared to influence the work reported in this paper.

AUTHORS' CONTRIBUTIONS

Nguyen Thi Thu Thuy and Vu Ngoc Phan designed the experiments and wrote the manuscript. Le Thi Le carried out all experiments.

ABBREVIATIONS

SMPs: Shape memory polymers
PU: Polyurethane
T_{trans}*: Transition temperature*
SMPU: Electrospun microfibers based on polyurethane
HA: Hydroxyapatite
DSC: Differential scanning calorimetry
DMF: N, N- Dimethyl formamide
EA: Ethyl acetate
SEM: Scanning Electron Microscopy
R_f*: Shape fixity*
R_r*: Shape recovery*
T_c*: Crystallization temperature*
T_g*: Glass temperature*
T_m*: Melting temperature*

REFERENCES

1. L S, WM H, and Zhao Y DZ, CC W, H P, C T. Stimulus-responsive shape memory materials: a review. Mater Des. 2012;33:577–640.
2. H L, X W, Y Y, J G, D H, B X, et al. Synergistic effect of siloxane modified aluminum nanopowders and carbon fiber on electrothermal efficiency of polymeric shape memory nanocomposite. Compos B Eng. 2015;80:1–6.
3. H L, M L, C Z, Y Y, J G, D H, et al. Controlling Au electrode patterns for simultaneously monitoring electrical actuation and shape recovery in shape memory polymer. Compos B Eng. 2015;80:37–42.
4. Shape-memory polymers. Mater Today. 2007;10(4):20–28.
5. P M, H S, C J, S R, K K. Thermosetting Shape Memory Polymers and Composites Based on Polybenzoxazine Blends, Alloys and Copolymers. Chem Asian J. 2019;14(23):4129–4139.
6. S H. Room-temperature-functional shape-memory polymers. Plast Eng. 1995;51(2):29–31.
7. M S, M NK, KM G, L U, K T, R M, et al. Characterization of polyurethane shape memory polymer and determination of shape fixity and shape recovery in subsequent thermomechanical cycles. Polymers. 2022;14(21):4775.
8. Polyurethane shape memory polymers. Boca Raton (FL): CRC Press. 2012;p. 20.
9. Q Y, G L. Investigation into stress recovery behavior of shape memory polyurethane fiber. J Polym Sci Part B Polym Phys. 2014;52(21):1429–1440.
10. J Y, H X, A T, QQ N. The effect of hydroxyapatite nanoparticles on mechanical behavior and biological performance of porous shape memory polyurethane scaffolds. J Biomed Mater Res Part A. 2018;106(1):244–254.
11. X L, Y N, KC C, S C. Rapid hemostatic and mild polyurethane-urea foam wound dressing for promoting wound healing. Mater Sci Eng C. 2017;71:289–297.
12. H L, D T, and Gao J SZ, X Y, S J, J P. Electrospun PCL-based polyurethane/HA microfibers as drug carrier of dexamethasone with enhanced biodegradability and shape memory performances. Colloid Polym Sci. 2020;298:103–111.
13. H M, T I, Y K, M M, A T, K R, et al. Shape-memory properties of electrospun non-woven fabrics prepared from degradable polyesterurethanes containing poly (ω-pentadecalactone) hard segments. Eur Polym J. 2012;48(11):1866–1874.
14. L T, L G, J H, Y Z, J H. Functional shape memory composite nanofibers with graphene oxide filler. Compos Part A Appl Sci Manuf. 2015;76:115–123.
15. N B, SC K. Electrospinning: A fascinating fiber fabrication technique. Biotechnol Adv. 2010;28(3):325–347.
16. Science and technology of polymer nanofibers. Hoboken (NJ): John Wiley & Sons. 2008;.
17. H Z, J H, S C, L Y. Preparation of polyurethane nanofibers by electrospinning. J Appl Polym Sci. 2008;109(1):406–411.
18. S B, M R, P R, A B, A EK. Preparation of electrospun shape memory polyurethane fibers in optimized electrospinning conditions via response surface methodology. Polym Adv Technol. 2020;31(10):2199–2208.
19. T S, K K, A L. Shape-memory properties of electrospun nonwovens prepared from amorphous polyetherurethanes under stress-free and constant strain conditions. MRS Online Proc Lib. 2012;1403:49–54.
20. C W, A B, S L. Effect of fiber diameter on tensile properties of electrospun poly (ε-caprolactone). Polymer. 2008;49(21):4713–4722.
21. T S, K K, M H, A L. Fiber diameter as design parameter for tailoring the macroscopic shape-memory performance of electrospun meshes. Mater Des. 2021;202(109546).
22. EPA K, Ç A, A Ç. Effects of β-cyclodextrin on selected properties of electrospun thermoplastic polyurethane nanofibres. Carbohydr Polyme. 2014;104:42–49.

23. Z-M H, YZ Z, M K, S R. A review on polymer nanofibers by electrospinning and their applications in nanocomposites. Compos Sci Technol. 2003;63(15):2223–2253.
24. A Ç, EPA K, Ç A. Effects of solvent mixtures on the morphology of electrospun thermoplastic polyurethane nanofibres. Textile and Apparel. 2015;25(1):38–46.
25. S R. An introduction to electrospinning and nanofibers. Singapore: World Scientific. 2005;.
26. T J, and Jitjaicham S HW, L W, M N, C P, C P, et al. Effect of solvents on electro-spinnability of polystyrene solutions and morphological apprarance of resulting electrospun polystyrene fibers. Eur Polym J. 2005;41:409–421.
27. uppatham C M, M N, P S. Ultrafine electrospun polyamide-6 fibers: effect of solution conditions on morphology and average fiber diameter. Macromol Chem Phys. 2004;205(17):2327–2338.
28. S K, IK K, T M. Structural features and mechanical properties of in situ–bonded meshes of segmented polyurethane electrospun from mixed solvents. J Biomed Mater Res Part B Appl Biomater. 2006;76(1):219–229.
29. TW S, DW L, SK L. Thermal and phase behavior of polyurethane based on chain extender, 2, 2-bis-[4-(2-hydroxyethoxy) phenyl] propane. Polym J. 1999;31(7):563–568.
30. G V, M B, A A, E Z. Estimating the degree of polymer stretching during electrospinning: An experimental imitation method. Macromol Mater Eng. 2017;302(1600554).
31. T C, A C, C H, E M, P C. 3D printed shape memory polymers produced via direct pellet extrusion. Micromachines. 2021;12(1):87.
32. Y S, H C, X G. High shape memory properties and high strength of shape memory polyurethane nanofiber-based yarn and coil. Polym Test. 2001;101(107277).
33. A L, A S, D L, S F, L P. Shape memory effect on electrospun PLA-based fibers tailoring their thermal response. Eur Polym J. 2019;117:217–226.
34. F Z, and Liu Y ZZ, J L. Shape memory properties of electrospun Nafion nanofibers. . Fiber Polym. 2014;15:534–539.
35. J A, M X, B Z, Y P, J S, Y Z, et al. Shape-memory performance of electrospun thermoplastic polyurethane/polyethylene oxide blend fibrous membranes with diverse morphological structures. . Polymer. 2023;288.
36. V S, A L, D L, JM K, L P. Shape-memory materials via electrospinning: A review. . Polymers . 2022;14:995.